single immunization with collagen, with an extremely low incidence (<10%, Fig. 4A) (*25*). Immunizing CD200$^{-/-}$ mice only once (*26*) resulted in disease onset as early as day 20 and a cumulative incidence of over 50% (Fig. 4A). That this result was not an artifact of gene targeting was illustrated by infecting C57BL/6$^{+/+}$ mice with a replication-deficient adenovirus expressing a soluble Ig-fusion protein of CD200R (*7*, *27*). Such mice were highly susceptible to CIA compared with mice receiving a control Ig-fusion protein construct (Fig. 4A). Both CD200$^{-/-}$ and CD200R-Ig–treated animals developed moderate to severe arthritis (*10*) with synovial inflammation and formation of invasive pannus, resulting in cartilage and bone degradation seen normally only in CIA-susceptible animals (*24*) (Fig. 4B). Inflammatory cells in the arthritic joints were mainly CD11b^{+} cells (*20*), with a substantial proportion being CD68^{+} macrophages (*10*).

Because EAE and CIA are initiated by activation of self-reactive T lymphocytes (*21*, *25*), enhanced disease could reflect hyperactivation of these cells in the absence of CD200. No evidence for T cell dysregulation in CD200-deficient environments was observed with a range of in vivo and in vitro experiments (*10*).

Thus, through CD200 expression, diverse tissues regulate macrophages, and probably also granulocytes, directly and continuously through interaction with the inhibitory CD200R (*7*). The consequences of loss of this pathway can be profound, rendering mice susceptible to tissue-specific autoimmunity and enabling accelerated reactivity of resident tissue macrophages, including those in the CNS. That these effects appear to be unrelated to T cell activation but rather the result of direct deregulation of effector pathways within the macrophage/myeloid lineage has important and broad implications for treatment of neurodegenerative diseases like Alzheimer's disease or for varied pathologies involving hyperactivation of the myeloid lineage.

References and Notes

1. HLDA7: 7th Workshop and Conference on Human Leukocyte Differentiation Antigens, Harrogate, UK, 20 to 24 June 2000.
2. A. N. Barclay, *Immunology* **42**, 727 (1981).
3. M. Webb, A. N. Barclay, *J. Neurochem.* **43**, 1061 (1984).
4. S. J. Davis *et al.*, *Immunol. Rev.* **163**, 217 (1998).
5. F. Borriello *et al.*, *Mamm. Genome* **9**, 114 (1998).
6. S. Preston *et al.*, *Eur. J. Immunol.* **27**, 1911 (1997).
7. G. J. Wright *et al.*, *Immunity* **13**, 233 (2000).
8. F. A. Lemckert, J. D. Sedgwick, H. Körner, *Nucleic Acids Res.* **25**, 917 (1997).
9. F. Köntgen *et al.*, *Int. Immunol.* **5**, 957 (1993).
10. Supplementary data are available at *Science* Online at www.sciencemag.org/cgi/content/full/290/5497/1768/DC1.
11. Single- and double-staining procedures used are detailed in (*28*). Primary antibodies were as in (*12*), and MOMA-1 (Bachem Bioscience, King of Prussia, PA), rabbit polyclonal anti-DAP12 antibody (*15*), and anti-CD45 (clone YTS165.1 obtained from S. P. Cobbold, University of Oxford, UK). Secondary antibodies were peroxidase- or alkaline phosphatase–conjugated polyclonal anti-rat or anti-rabbit IgG (Jackson Immunochemicals, NJ). Hind limbs for histological analysis were prepared by means of a procedure adapted from (*29*).
12. Single-cell suspensions of spleens were stained for mCD200 (*13*), B220, CD4, CD8, CD11b, Ly-6G, and F4/80 (PharMingen, San Diego, CA, and Caltag, Burlingame, CA) by standard procedures.
13. OX90 was prepared by fusing splenocytes from rats immunized with a mouse CD200–rat CD4 fusion protein (*6*) with the Y3 myeloma, by standard procedures. The monoclonal antibody was selected by its capacity to bind recombinant mCD200–rat CD4 in an enzyme-linked immunosorbent assay (ELISA) and to bind those cells predicted to express CD200 (*2*, *3*).
14. G. Kraal, M. Janse, *Immunology* **58**, 665 (1986).
15. A. B. H. Bakker *et al.*, *Immunity* **13**, 345 (2000).
16. V. H. Perry, S. Gordon, *Trends Neurosci.* **11**, 273 (1988).
17. J. D. Sedgwick *et al.*, *Proc. Natl. Acad. Sci. U.S.A.* **88**, 7438 (1991).
18. G. W. Kreuzberg, *Glia* **19**, 312 (1996).
19. M. B. Graeber, W. J. Streit, G. W. Kreutzberg, *J. Neurosci. Res.* **21**, 18 (1988).
20. R. M. Hoek *et al.*, data not shown.
21. C. S. Raine, *Lab. Invest.* **50**, 608 (1984).
22. S. R. McColl, *et al.*, *J. Immunol.* **161**, 6421 (1998).
23. EAE was induced and scored as described in (*30*) by subcutaneous immunization with 50 μg of myelin oligodendrocyte glycoprotein (MOG)$_{35-55}$ peptide in complete Freund's adjuvant (CFA), but each mouse received 0.1 mg of H37RA *Mycobacterium tuberculosis* and intravenous injections of 100 ng of pertussis toxin on the day of immunization and 2 days later.
24. I. K. Campbell *et al.*, *Ann. Rheum. Dis.* **56**, 364 (1997).
25. W. C. Watson, A. S. Townes, *J. Exp. Med.* **162**, 1878 (1985).
26. CIA was induced by immunization intradermally with 100 μg of chicken type II collagen in CFA (0.25 mg H37RA *M. tuberculosis*) and scored only by clinical criteria as described in (*24*).
27. The adapted mCD200R cDNA (residues 86 to 720) was subcloned in the Xho I site of a modified pCDM8.Ig expression plasmid (*31*). The Hind III–Not I fragment of this was transferred to a modified pQB1-AdCMV5-GFP adenovirus transfer vector (Quantum Biotechnologies, Montreal, Canada), with an additional multicloning site 5′-AGATCTAAGCTTGCACGCGTATGCGGCCGCATGGTACCATTCTAGAGCGATATCGTTTAA AC-3′ added between the Bgl II and Pme I sites. Recombinant adenovirus was produced with host QBI-293A human embryonic kidney cells (Quantum applications manual 24AL98). Virus expressing only the human Fc portion encoded by pCDM8.Ig was used as control. Mice were infected 5 days before collagen immunization, and serum human Ig levels were subsequently monitored by ELISA.
28. J. D. Sedgwick *et al.*, *J. Exp. Med.* **177**, 1145 (1993).
29. R. Jonsson, A. Tarkowski, L. Klareskog, *J. Immunol. Methods* **88**, 109 (1986).
30. D. S. Riminton *et al.*, *J. Exp. Med.* **187**, 1517 (1998).
31. E. E. Bates *et al.*, *Mol. Immunol.* **35**, 513 (1998).
32. At various times after facial nerve transection (*19*), tissue was prepared for immunohistochemistry (*11*) of the brainstem area containing nucleus VII. To ensure valid comparison between different tissues, we made 20-μm coronal sections in a caudo-rostral direction starting in the cervical spinal cord, and advancing until the first appearance of nucleus VII. Eight-micrometer serial sections were prepared, and microglial activation was assessed (*11*, *19*).

33. We thank F. A. Lemckert and D. S. Riminton (Centenary Institute, Sydney, Australia) for technical assistance, N. Hutchings (University of Oxford, UK) for analysis of OX90 mAb, and L. Spargo (Hanson Centre, Adelaide, Australia) for advice on preparation of CIA tissue. We thank L. L. Lanier (UCSF, CA) and A. B. H. Bakker (DNAX, CA) for DAP12 antiserum, S. Gordon (University of Oxford, UK) for CD68 mAb, Y.-J. Liu (DNAX, CA) for support with DC studies, and M. Andonion for graphics assistance. Co-workers in Oxford were supported by the UK Medical Research Council. DNAX Research Institute is supported by Schering Plough Corporation.

14 August 2000; accepted 27 October 2000

Accumulation of Dietary Cholesterol in Sitosterolemia Caused by Mutations in Adjacent ABC Transporters

Knut E. Berge,[1]* Hui Tian,[3]* Gregory A. Graf,[1] Liqing Yu,[1] Nick V. Grishin,[2] Joshua Schultz,[3] Peter Kwiterovich,[4] Bei Shan,[3] Robert Barnes,[1] Helen H. Hobbs[1]†

In healthy individuals, acute changes in cholesterol intake produce modest changes in plasma cholesterol levels. A striking exception occurs in sitosterolemia, an autosomal recessive disorder characterized by increased intestinal absorption and decreased biliary excretion of dietary sterols, hypercholesterolemia, and premature coronary atherosclerosis. We identified seven different mutations in two adjacent, oppositely oriented genes that encode new members of the adenosine triphosphate (ATP)–binding cassette (ABC) transporter family (six mutations in *ABCG8* and one in *ABCG5*) in nine patients with sitosterolemia. The two genes are expressed at highest levels in liver and intestine and, in mice, cholesterol feeding up-regulates expressions of both genes. These data suggest that ABCG5 and ABCG8 normally cooperate to limit intestinal absorption and to promote biliary excretion of sterols, and that mutated forms of these transporters predispose to sterol accumulation and atherosclerosis.

In humans, the intestine presents a barrier that prevents the absorption of plant sterols and partially blocks the absorption of cholesterol. This barrier is disrupted in the rare autosomal recessive disorder, sitosterolemia, which is characterized by hyperabsorption of plant sterols such as sitosterol (*1–3*). Patients with sitosterolemia also hyperabsorb cholesterol and are usually hypercholesterolemic, which leads to the development of xanthomas (cholesterol deposits in skin and tendons) and premature coronary artery disease (*2–5*). Unlike individuals with other forms of hyperlipidemia, sitosterolemic subjects respond to restriction in dietary cholesterol and to bile acid resin treatment with dramatic reductions in plasma cholesterol levels (*2*, *3*, *6*).

Patients with sitosterolemia have markedly elevated (>30-fold) plasma levels of plant sterols (sitosterol, stigmasterol, and campesterol) as well as other neutral sterols with modified side chains (*1*, *7*, *8*). Healthy individuals absorb only ~5% of the average 200 to 300 mg of plant sterols consumed each day (*9*). Almost all of the absorbed sitosterol is quickly secreted into the bile so that only trace amounts of sitosterol and other plant sterols remain in the blood (*9*). In contrast, subjects with sitosterolemia absorb between 15 and 60% of ingested sitosterol, and they excrete only a fraction into the bile (*2–5*). The liver secretes sitosterol into the bloodstream, where it is transported as a constituent of low-density and high-density lipoprotein particles (*1*). With the exception of the brain, the relative proportion of sterol represented by sitosterol in tissues matches that in plasma (10 to 25%) (*10*). Hyperabsorption and inefficient secretion are not limited to plant sterols. Sitosterolemic subjects absorb a higher fraction of dietary cholesterol than normal subjects, and they secrete less cholesterol into the bile (*2–5*). Taken together, the genetic and metabolic data indicate that sitosterolemic patients lack a gene product that normally limits the absorption and accelerates the biliary excretion of sterols (*2*, *3*).

The molecular mechanisms that limit sterol absorption are poorly understood, but clues have emerged recently from studies of the orphan nuclear hormone receptor LXR (*11*, *12*). Mice treated with an LXR agonist show a marked decrease in cholesterol absorption and a corresponding increase in the intestinal expression of mRNA encoding the ATP-binding cassette protein–1 (ABCA1), a membrane-associated protein that has been implicated in the transport of cholesterol (*11*, *13*). We hypothesized that sitosterolemic patients might have defects in other genes that limit cholesterol absorption and that the expression of these genes would be regulated by LXR. To test this idea, we used DNA microarrays to search for mRNAs that are induced by the LXR agonist T091317 in mouse liver and intestine (*11*, *14*). A transcript corresponding to a murine EST (AA237916) was induced ~2.5-fold in the livers and intestines of treated mice. This EST resembled three *Drosophila* genes that encode ABC half-transporters (*brown*, *scarlet*, and *white*) expressed in the pigmentary cells of the eye (*15–17*). These ABC half-transporters contain six membrane-spanning domains and form two types of heterodimers that transport guanine (*brown/white*) or tryptophan (*scarlet/white*). Because a human homolog of *white* (*ABCG1*) is implicated in cellular cholesterol efflux from macrophages (*18*, *19*), we reasoned that the LXR-induced protein encoded by AA237916 might be involved in sterol trafficking in liver and intestine, and hence this gene was a candidate for the defect in sitosterolemia.

A full-length cDNA corresponding to

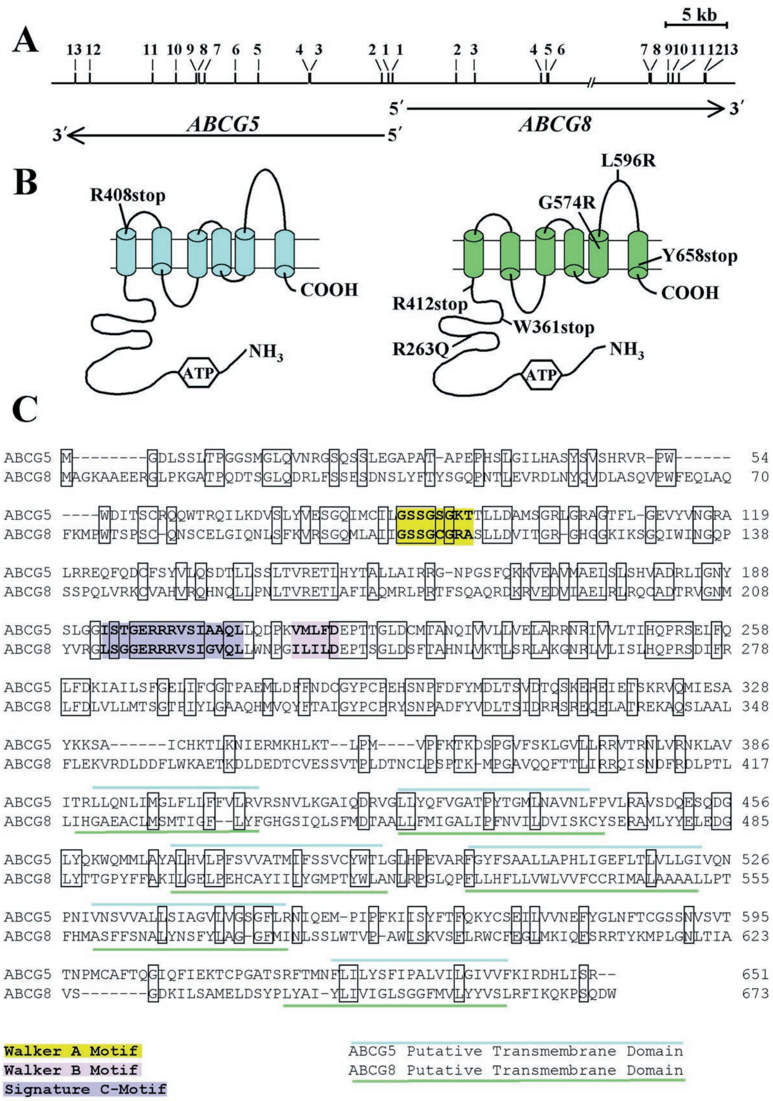

Fig. 1. Genomic structure (**A**), putative topology (**B**), and predicted amino acid sequences of ABCG5 and ABCG8 (**C**). *ABCG5* and *ABCG8* are located on chromosome 2p21 between markers D2S177 and D2S119. (A) *ABCG5* and *ABCG8* are tandemly arrayed in a head-to-head orientation separated by 374 base pairs. *ABCG5* and *ABCG8* are both encoded by 13 exons and each spans ~28 kb. (B) The mutations detected in patients with sitosterolemia (Table 1) are indicated on a schematic model of *ABCG5* (left) and *ABCG8* (right). (C) Predicted amino acid sequence of ABCG5 and ABCG8, which are 651 and 673 residues in length, respectively. Alignment of the inferred amino acid sequences indicates 28% sequence identity and 61% sequence similarity between ABCG5 and ABCG8. Both proteins are predicted to contain six transmembrane segments (*22*). The putative transmembrane segments of each protein are indicated by blue (ABCG5) or green (ABCG8) cylinders (B) and lines (C). The Walker A and Walker B motifs are highlighted in yellow and lavender, respectively. The ABC signature sequence (C motif) is indicated in purple.

[1]Department of Molecular Genetics and McDermott Center for Human Growth and Development and [2]Howard Hughes Medical Institute and Department of Biochemistry, University of Texas Southwestern Medical Center at Dallas, 5323 Harry Hines Boulevard, Dallas, TX 75390–9046, USA. [3]Tularik Inc., Two Corporate Drive, South San Francisco, CA 94080, USA. [4]Department of Pediatrics, Johns Hopkins University, Baltimore, MD 21205, USA.

*These authors contributed equally to the work.
†To whom correspondence should be addressed: Helen.Hobbs@UTSouthwestern.edu

AA237916 was isolated from a mouse liver cDNA library (OriGene Technologies, Rockville, Maryland), and this sequence was used to identify a human ortholog in the GenBank EST database (T86384). A full-length human sequence was obtained by iterative EST database searches and by cloning from human liver cDNA libraries (OriGene and Clontech, Palo Alto, California). The human cDNA predicts a 651–amino acid protein (Fig. 1C) that shares 80% sequence identity with the mouse sequence (*20*). Following the standard system of nomenclature in the ABC transporter field, this protein was named ABCG5. The amino-terminal half of ABCG5 contains the ATP-binding motifs (Walker A and B motifs) and an ABC-transporter signature motif (C motif), and the carboxyl-terminal region is predicted to contain six transmembrane (TM) segments (Fig. 1B) (*17*, *21*, *22*). A human EST clone (UniGene T93792) from *ABCG5* mapped to chromosome 2p21 between markers D2S177 and D2S119, and the map position was confirmed using a radiation hybrid panel (*23*). Patel and colleagues previously mapped the human sitosterolemia gene to this same region of chromosome 2 in ten independent sitosterolemic families (*24*).

The structure of the human *ABCG5* gene was characterized by analysis of a bacterial artificial chromosome (BAC) clone that contained the entire gene (Fig. 1A) (*25*). The gene spans ~28 kb and has 13 exons and 12 introns. The coding sequences and consensus splicing sequences were amplified from genomic DNA by polymerase chain reaction (PCR) and sequenced in nine unrelated subjects with sitosterolemia (Table 1). A sitosterolemic patient from Hong Kong (proband 9) was heterozygous for a transition mutation (<u>C</u>GA to <u>T</u>GA) in codon 408 that introduced a premature stop codon between TM1 and TM2. This mutation was not present in 65 normolipidemic individuals, including 50 Chinese subjects. No other potential disease-causing mutations were identified in *ABCG5*. A transversion in codon 604 that substituted a glutamic acid for glutamine (Q604E) in the loop between TM5 and TM6 was found in five sitosterolemic probands but was also present in 23% of the alleles from normolipidemic Caucasians ($n = 50$).

Genes encoding members of the ABC transporter family are often clustered in the genome (*26*). Because only a single *ABCG5* mutation was identified in our collection of nine sitosterolemic probands, we searched the public and Celera genome sequences for other ABC transporters adjacent to *ABCG5*. An EST (T84531) that shared weak homology with the *Drosophila white* gene was identified and expanded using exons predicted by the computer program GENSCAN (*27*). Eleven of the 13 exons of the new gene, which we name *ABCG8*, were identified in the databases, and the remaining two exons were identified by sequencing PCR-amplified cDNAs from human hepatic poly(A)$^+$ mRNA. ABCG8 shares ~28% amino acid identity with ABCG5 (Fig. 1C). The *ABCG8* sequence is most similar to *ABCG1*, which resembles the *Drosophila white* gene (*16*).

The translational start sites of *ABCG5* and *ABCG8* are separated by only 374 base pairs, and the two genes are arranged in a head-to-head orientation (Fig. 1A). Both genes contain a translation initiation codon with an upstream in-frame stop codon. The close proximity and opposite orientation of *ABCG5* and *ABCG8* suggest that the two genes have a bidirectional promoter and share common regulatory elements (*28*, *29*). No obvious LXR response element was identified in the limited amount of sequence available at this time. Other gene pairs with bidirectional promoters form functional complexes (*29*), as may be the case for ABCG5 and ABCG8.

The predicted intron-exon boundaries of human *ABCG8* were confirmed by DNA sequencing. The single-strand conformation polymorphism (SSCP) technique was used to screen the exons and flanking intron sequences of *ABCG8* in the nine sitosterolemic subjects (Table 1) (*30*, *31*). DNA sequencing of abnormally migrating fragments revealed six different mutations (Table 1 and Fig. 1B). The first patient to be described with sitosterolemia (proband 1) was homozygous for a nonsense mutation (1083G>A) in exon 7 (Fig. 1B) that introduced a premature termination signal codon at codon 361, terminating the protein before TM1 (*1*). Three other unrelated Caucasian sitosterolemic subjects (probands 3, 5, and 8) were heterozygous for the same mutation (*6*, *32*). One of these probands (proband 5) was originally diagnosed with pseudohomozygous familial hypercholesterolemia (FH), an autosomal recessive disorder characterized by hypercholesterolemia, tendon xanthomas, and exquisite sensitivity to dietary cholesterol (*6*). Many of the patients originally diagnosed with pseudohomozygous FH were subsequently found to have sitos-

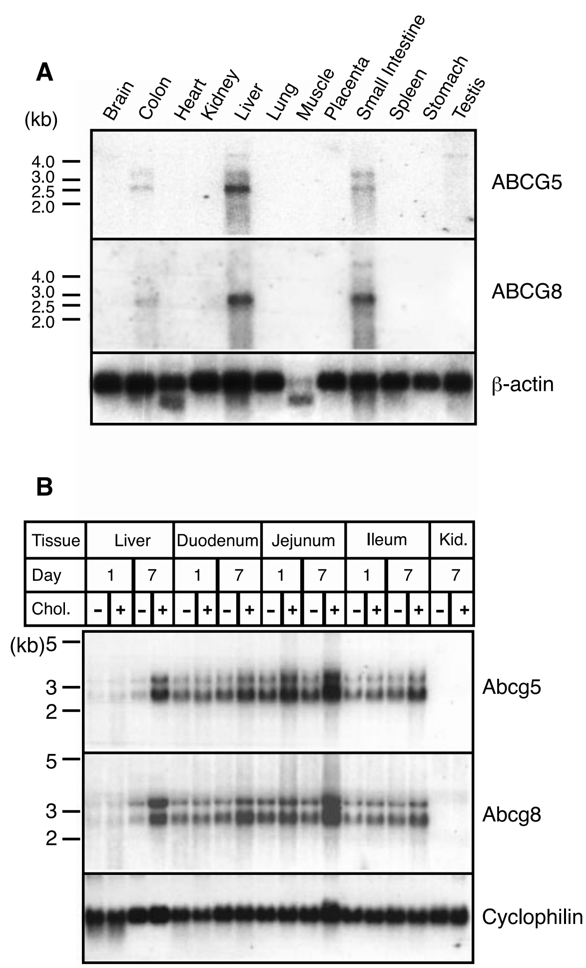

Fig. 2. Expression of *ABCG5* (AF320293) and *ABCG8* (AI320294) in human tissues (**A**) and the effect of cholesterol feeding on levels of *ABCG5* and *ABCG8* mRNAs in mouse liver and intestine (**B**). (A) Northern blot analysis of human tissues. The coding sequence of *ABCG5* and *ABCG8* were amplified from liver poly(A)$^+$ RNA (Clontech), and the fragments were cloned into the plasmid vector pGEM-T (Promega, Madison, Wisconsin). The coding region of *ABCG5* and the 3′-untranslated region of *ABCG8* was amplified and the fragment radiolabeled (Megaprime DNA labeling System, Amersham, Uppsala) before incubation with the RNA blot (OriGene) in Rapid-hyb buffer (1×10^6 cpm/ml) (Amersham). The blot was washed and subjected to autoradiography for 18 hours using Kodak X-OMAT-blue film (Kodak, Rochester, New York) (*40*). (B) Cholesterol feeding induces coordinate increases in levels of *Abcg5* and *Abcg8* mRNA. Seven-week-old male mice (129S3/SvImj) were fed powdered rodent diet (Harlan Teklad, Madison, Wisconsin) in the absence or presence of cholesterol (2%, w/v). Mice were killed after 1 or 7 days in the light phase of a 12-hour dark-light cycle. Total RNA was isolated using RNA–Stat-60 (Tel-Test, Friendsword, Texas) from the liver and three equal segments of the small intestine (duodenum, jejunum, and ileum). The tissue RNAs were pooled from three animals, and aliquots (15 μg) were used to make duplicate Northern blots (*40*). The mouse cDNAs for *Abcg5* and *Abcg8* were used as probes. Cyclophilin was used as an internal standard. The results were identical when probes generated from the 3′ untranslated regions of both cDNAs were used.

terolemia, as was the case with this patient and proband 6 (*6*, *33*). Proband 3 was heterozygous for another nonsense mutation in exon 13 that introduced a stop codon 15 residues from the carboxyl terminus of ABCG8. The resulting protein would lack part of TM6 and the short cytoplasmic domain, which contains a cluster of positively charged residues that may be important in positioning these proteins in the membrane (*34*).

Two missense mutations identified in *ABCG8* produced nonconservative amino acid changes at positions that are conserved between the humans and mouse proteins, as well as in ABCG5. One Chinese patient (proband 4) was heterozygous for a missense mutation in exon 6 in codon 263 (Glu for Arg, R263Q). An Amish individual with sitosterolemia was homozygous for a missense mutation (Arg for Gly, G574R) in a residue that is conserved in mouse and human ABCG8. Genomic DNA was available from an additional three of the four living affected family members in this large Amish pedigree (*35*, *36*), and these individuals were homozygous for this same missense mutation (*20*). A third nonconservative missense mutation was an arginine substitution for a leucine at codon 596. The corresponding sequence in ABCG5 is another nonpolar amino acid, glutamine. None of these three missense mutations were identified in 100 alleles from ethnically matched normolipidemic subjects, which is consistent with their being disease-causing mutations. A common polymorphism (Cys for Tyr, Y54C) with an allele frequency of 23% in control subjects (n = 100 alleles) was also identified in *ABCG8*.

Thus, we identified two mutant alleles at the *ABCG8* locus in four of the nine sitosterolemic patients. Four patients had a single mutant allele in *ABCG8*, and one patient had a single mutant allele in *ABCG5*. The identification of multiple different *ABCG8* mutations in subjects with sitosterolemia, including nonsense mutations that appear incompatible with protein function, provides strong evidence that sitosterolemia is caused by defects in this gene. It also seems likely that the mutation we found in *ABCG5* causes sitosterolemia, although the identification of additional mutations in this gene will be required to substantiate this hypothesis. It remains possible that mutations in another gene (perhaps a different ABC transporter) within the genomic interval mapped by Patel *et al.* (*24*) can cause sitosterolemia when present in combination with mutations in *ABCG5* or *ABCG8*.

To determine whether *ABCG5* and *ABCG8* are regulated coordinately, we examined the tissue distributions of their mRNAs in humans and mice, and their responses to cholesterol feeding in mice. In humans, liver and the small intestine were the major sites of expression of both genes (Fig. 2A). For both *ABCG5* and *ABCG8*, one major transcript of 2.4 kb and 2.6 kb, respectively, but other transcripts were visible by RNA blotting. Additional studies will be required to determine the identity of these transcripts, which presumably result from alternative splicing or differential polyadenylation. In mice, *Abcg5* and *Abcg8* were expressed at higher levels in the intestine than in the liver, although the relative amounts of expression in these two tissues may be strain-specific. Inasmuch as the expression of these two genes is regulated by dietary sterols (see below), definitive studies of tissue expression in humans will require careful control of dietary intake.

If *ABCG5* and *ABCG8* protect against the accumulation of sterols, then their expression levels would be predicted to increase with cholesterol feeding. To test this hypothesis, we fed mice a high-cholesterol diet (2%), and they were killed after 1, 7, or 14 days. The levels of *Abcg5* and *Abcg8* mRNAs increased about twofold in intestine and over threefold in liver within 1 week of initiation of the high-cholesterol diet (Fig. 2B). These changes were maintained at 2 weeks (*20*). As expected, the plasma levels of cholesterol did not significantly change in the cholesterol-fed mice (from 95 mg/dl to 93 mg/dl), because mice rapidly and efficiently convert dietary cholesterol into bile acids and excrete both cholesterol and bile acids into the bile (*37*). LXR plays a central role in this regulated process by increasing the expression of multiple hepatic genes that promote bile acid synthesis and biliary secretion (*12*). The ligands for LXR include hydroxylated sterols that are derived from cholesterol (*38*, *39*). Because *ABCG5* is induced by an LXR agonist, it is possible that dietary sterols induce these genes through LXR.

In summary, our data suggest that ABCG5 and ABCG8 are ABC half-transporters that may partner to generate a functional protein. The juxtaposition of the corresponding genes on chromosome 2, the coordinate regulation of their mRNAs in the liver and intestine with cholesterol feeding, and the observation that mutations in either gene are associated with sitosterolemia suggest that these two proteins form a functional complex that mediates efflux of dietary cholesterol from the intestine, and thus protects humans from sterol overaccumulation. This protection is especially important in Western societies that consume high-cholesterol diets. Loss of function of these proteins causes sitosterolemia. Our results raise the possibility that subtle defects in these proteins or in their regulation may underlie the variable responses of healthy individuals to high-cholesterol diets.

Note added in proof: After submission of

Table 1. Molecular defects in nine unrelated individuals with sitosterolemia. Genomic DNA was extracted from cultured fibroblasts or lymphoblasts from the proband or another family member with sitosterolemia (*31*). All subjects had elevated plasma sitosterol levels (except proband 6 in which plasma sitosterol level was not measured). The age at the time of diagnosis or at the first appearance of xanthomas is provided (when available). The exons and flanking splice site consensus sequences were screened for sequence variations using SSCP and dideoxy-sequencing (*31*). None of the mutations were found in 100 alleles from normolipidemic controls. The nucleotides are numbered consecutively starting at the A of the initiation codon ATG. Plasma cholesterol levels were obtained from referring physicians or from publications. Abbreviations: ref., reference; yr, years; C, fasting plasma cholesterol level; chol., cholesterol; CAD, coronary artery disease; mo, months; LDL, low density lipoprotein; NI, not identified; amino acids: G, Gly; Q, Gln; L, Leu, P, Pro; R, Arg; T, Thr; W, Trp; Y, Tyr.

Patient (age)	Ethnicity	Mutant alleles	Nucleotide change	Amino acid change(s)	Comments	Ref.
1 (8 yr)	German/Swiss	*ABCG8* *ABCG8*	1083G>A 1083G>A	W361Stop W361Stop	Original case. C = 195 mg/dl	(*1*)
2 (13 yr)	Amish American	*ABCG8* *ABCG8*	1720G>A 1720G>A	G574R G574R	13-year-old died of CAD	(*35*)
3 (8 mo)	Caucasian American	*ABCG8* *ABCG8*	1083G>A 1974C>G	W361Stop Y658Stop	C fell from 800 to 151 mg/dl on low-chol. diet	
4 (<10 yr)	Chinese	*ABCG8* NI	788G>A NI	R263Q NI	C = 556 mg/dl	
5 (5 yr)	Caucasian American	*ABCG8* *ABCG8*	1083G>A 1234C>T	W361Stop R412Stop	C fell from 375 to 201 mg/dl on low-chol. diet	(*6*)
6 (2 yr)	Caucasian American	*ABCG8* NI	1787T>G NI	L596R NI	C fell from 753 to 106 mg/dl on low-chol. diet	(*33*)
7	Mexican-American	*ABCG8* NI	1234C>T NI	R412Stop NI	LDL-C fell from 380 to 200 mg/dl	
8 (3.5 yr)	Caucasian New Zealander	*ABCG8* NI	1083G>A NI	W361Stop NI	C fell from 718 to 127 mg/dl on low-chol. diet	(*32*)
9 (<10 yr)	Chinese	*ABCG5* NI	1222C>T NI	R408 Stop NI	C = 620 mg/dl	

the manuscript two additional mutations in *ABCG8* were identified by sequencing: (i) del547C resulting in a premature stop codon at amino acid 191 in proband 7 and (ii) P231T (691 A>C) in proband 4. No additional mutations were identified in *ABCG5*.

References and Notes

1. A. K. Bhattacharyya, W. E. Connor, *J. Clin. Invest.* **53**, 1033 (1974).
2. I. Bjorkhem, K. M. Boberg, in *The Metabolic and Molecular Bases of Inherited Disease*, C. R. Scriver, A. L. Beaudet, W. S. Sly, D. Valle, Eds. (McGraw-Hill, New York, ed. 7, 1995), vol. 2, chap. 65, p. 2073.
3. G. Salen *et al.*, *J. Lipid Res.* **33**, 945 (1992).
4. T. A. Miettinen, *Eur. J. Clin. Invest.* **10**, 27 (1980).
5. D. Lutjohann, I. Bjorkhem, V. F. Beil, K. von Bergmann, *J. Lipid Res.* **36**, 1763 (1995).
6. I. Morganroth, R. I. Levy, A. E. McMahon, A. M. Gotto Jr., *J. Pediatr.* **85**, 639 (1974).
7. G. Salen *et al.*, *J. Lipid Res.* **26**, 203 (1985).
8. R. E. Gregg, W. E. Connor, D. S. Lin, H. B. Brewer Jr., *J. Clin. Invest.* **77**, 1864 (1986).
9. G. Salen, E. H. Ahrens Jr., S. M. Grundy, *J. Clin. Invest.* **49**, 952 (1970).
10. G. Salen *et al.*, *J. Lipid Res.* **26**, 1126 (1985).
11. J. J. Repa *et al.*, *Science* **289**, 1524 (2000).
12. D. J. Peet *et al.*, *Cell* **93**, 693 (1998).
13. R. M. Lawn *et al.*, *J. Clin. Invest.* **104**, 25 (1999).
14. Total RNA was prepared from the liver, intestine, and kidney of C57BL/6mice treated with the LXR agonist T091317 (50 mg/kg). Duplicate RNA samples were labeled with two fluorescent dyes and hybridized to mouse GEM1 microarrays (performed at Incyte Genomics, Palo Alto, CA).
15. D. T. Sullivan, S. L. Grillo, R. J. Kitos, *J. Exp. Zool.* **188**, 225 (1974).
16. P. M. Bingham, R. Lewis, G. M. Rubin, *Cell* **25**, 693 (1981).
17. C. Higgins, *Annu. Rev. Cell Biol.* **8**, 67 (1992).
18. J. Klucken *et al.*, *Proc. Natl. Acad. Sci. U.S.A.* **97**, 817 (2000).
19. A. Venkateswaran *et al.*, *J. Biol. Chem.* **275**, 147000 (2000).
20. K. E. Berge *et al.*, unpublished observations.
21. J. E. Walker, M. Saraste, M. J. Runswick, N. J. Gay, *EMBO J.* **1**, 945 (1982).
22. D. T. Jones, W. R. Taylor, J. M. Thornton, *Biochemistry* **33**, 3038 (1994).
23. Chromosomal localization of *ABCG5* was confirmed by using primers derived from exon 7 of *ABCG5* to amplify a gene-specific fragment from the TNG panel of radiation hybrids from Stanford Human Genome Center (Research Genetics, Inc.). The result was submitted to the RH Server (http://www-shgc.stanford.edu/RH/index.html), which linked *ABCG5* to SHGC14952, which is between markers D2S177 and D2S119.
24. S. B. Patel *et al.*, *J. Clin. Invest.* **102**, 1041 (1998).
25. The last three exons of *ABCG5* were contained in the GenBank sequence entry AC011242 and were further confirmed by PCR analysis from human genomic DNA. The remaining 10 exon/intron boundaries were determined by using PCR and cDNA primers to amplify the exon sequences and the intron/exon boundaries by using genomic DNA and cDNA primers followed by sequence analysis.
26. O. Le Saux *et al.*, *Nature Genet.* **25**, 223 (2000).
27. The 3′ end of *ABCG5* was located on BAC RP11-489K22, which had been partially sequenced, but no other ABC transporters were identified on this BAC. A BAC end sequence (BES) in the Genome Survey Sequence database that was located on BAC RP11-489K22 was used to search the Celera Human Fragments database. The public and Celera databases were used to assemble most of the genomic sequences in the region, resulting in the identification of EST T84531, which shared weak homology with the *Drosophila white* gene (*16*). The GENSCAN Web Server (http://genes.mit.edu/GENSCAN.html) was used to identify additional exons within this gene. The sequence of the ~30-kb region was assembled (excluding three gaps) using the Celera Human Fragments database and mouse ESTs in the public database.
28. S. A. Ikeda, A. Mochizuki, A. H. Sarker, S. Seki, *Biochem. Biophys. Res. Commun.* **273**, 1063 (2000).
29. R. Pollner, C. Schmidt, G. Fischer, K. Kuhn, E. Poschl, *FEBS Lett.* **405**, 31 (1997).
30. M. Orita, Y. Suzuki, T. Sekiya, K. Hayashi, *Genomics* **5**, 874 (1989).
31. H. H. Hobbs, M. S. Brown, J. L. Goldstein, *Hum. Mutat.* **1**, 445 (1992).
32. E. R. Nye, W. H. Sutherland, J. G. Mortimer, H. C. Stringer, *N. Z. Med. J.* **101**, 418 (1988).
33. P. S. Stell, D. L. Sprecher, *Top. Clin. Nutr.* **5**, 63 (1990).
34. G. D. Ewart, D. Cannell, G. B. Cox, A. J. Howells, *J. Biol. Chem.* **269**, 10370 (1994).
35. P. O. Kwiterovich Jr. *et al.*, *Lancet* **i**, 466 (1981).
36. T. H. Beaty *et al.*, *Am. J. Hum. Genet.* **38**, 492 (1981).
37. D. W. Russell, K. D. Setchell, *Biochemistry* **31**, 4737 (1992).
38. B. A. Janowski *et al.*, *Nature* **383**, 728 (1996).
39. B. A. Janowski *et al*, *Proc. Natl. Acad. Sci. U.S.A.* **96**, 266 (1999).
40. V. Jokinen *et al.*, *J. Biol. Chem.* **269**, 26411 (1994).
41. We wish to thank T. Hyatt, Y. Liao, L. Beatty, B. P. Crider, D. Virgil, R. Wilson, S. Niu, J. Wu, S. Padmanabhan, and M. Rich for excellent technical assistance; T. DiSessa, A. Gotto, J. Kane, L. C. K. Low, and E. R. Nye for providing tissue samples from patients with sitosterolemia; and M. S. Brown and J. L. Goldstein for making the samples available to us and for helpful discussions. We thank D. W. Russell for manuscript review and helpful discussions. Supported by NIH grant HL20948, the W. M. Keck and the W. R. Reynolds Foundations, the Norwegian Research Council (K.E.B.), and NIH training grant HL07360 (G.A.G).

19 October 2000; accepted 31 October 2000

From Marrow to Brain: Expression of Neuronal Phenotypes in Adult Mice

Timothy R. Brazelton, Fabio M. V. Rossi, Gilmor I. Keshet, Helen M. Blau*

After intravascular delivery of genetically marked adult mouse bone marrow into lethally irradiated normal adult hosts, donor-derived cells expressing neuronal proteins (neuronal phenotypes) developed in the central nervous system. Flow cytometry revealed a population of donor-derived cells in the brain with characteristics distinct from bone marrow. Confocal microscopy of individual cells showed that hundreds of marrow-derived cells in brain sections expressed gene products typical of neurons (NeuN, 200-kilodalton neurofilament, and class III β-tubulin) and were able to activate the transcription factor cAMP response element–binding protein (CREB). The generation of neuronal phenotypes in the adult brain 1 to 6 months after an adult bone marrow transplant demonstrates a remarkable plasticity of adult tissues with potential clinical applications.

Until recently, the fate of adult cells has been thought to be restricted to their tissues of origin. Cells are well known to be capable of replenishing damage in tissues in which they reside, such as blood, muscle, liver, and skin. However, the finding that adult cells could be reprogrammed to express genes typical of differentiated cell types representing all three lineages (mesoderm, endoderm, and ectoderm) when fused to cells in heterokaryons was quite unexpected (*1–3*). This degree of plasticity demonstrated that the differentiated state is reversible and requires continuous regulation to maintain the balance of factors present in a cell at any given time (*4*). The cloning of frogs (*5*) and later sheep (*6*) further showed that previously silent genes could be activated in adult nuclei. Although remarkable, these examples of plasticity all involved extensive experimental manipulations. More recently, findings have been made that suggest that stem cells can assume diverse fates under physiologic conditions. Both transformed and primary neural cells can give rise to a range of phenotypes typical of their site of implantation within the central nervous system (CNS) (*7*, *8*). Bone marrow cells can yield not only all cells of the blood but also cells with a liver phenotype (*9*). Perhaps the greatest plasticity yet demonstrated is the "homing" of bone marrow–derived cells to damaged muscle in irradiated dystrophic *mdx* mice (*10*, *11*). Muscle-derived and CNS-derived stem cell–like populations have also been reported to reconstitute the blood and rescue lethally irradiated mice (*11*, *12*). Here we report that after lethal irradiation, bone marrow–derived cells administered by intravascular injection yielded cells that expressed genes specific to neurons (neuronal phenotypes) in the CNS. Moreover, both the sources and the recipients of these cells were adults.

To examine whether bone marrow–derived cells could give rise to cells in the brain, adult marrow was harvested from transgenic

Department of Molecular Pharmacology, CCSR 4215, 269 Campus Drive, Stanford University, Stanford, CA 94305–5175, USA.

*To whom correspondence should be addressed. E-mail: hblau@stanford.edu